# Monolithically Integrated Photonic Structures for Stable On-Chip Solar Blind Communications

HE Rui[1,2], HU Qiang[1,2], RAN Junxue[1,2], WANG Junxi[1,2], WEI Tongbo[1,2]

(1. Research and Development Center for Wide Bandgap Semiconductors, Institute of Semiconductors, Chinese Academy of Sciences, Beijing 100083, China；
 2. Center of Materials Science and Optoelectronics Engineering, University of Chinese Academy of Sciences, Beijing 100049, China)

**Abstract:** A solar-blind multi-quantum well (MQW) structure wafer based on AlGaN materials is epitaxial growth by metal-organic chemical vapor deposition (MOCVD). The monolithically integrated photonic chips including light-emitting diodes (LEDs), waveguides, and photodetectors (PDs) are presented. The results of the finite-difference time-domain (FDTD) simulation confirm the strong light constraint of the waveguide designed with the triangular structure in the optical coupling region. Furthermore, in virtue of predominant ultraviolet transverse magnetic (TM) modes, the solar blind optical signal is more conducive to lateral transmission along the waveguide inside the integrated chip. The integrated PDs demonstrate sufficient photosensitivity to the optical signal from the integrated LEDs. When the LEDs are operated at 100 mA current, the photo-to-dark current ratio (PDCR) of the integrated PD is about seven orders of magnitude. The responsivity, specific detectivity, and external quantum efficiency of the integrated self-driven PD are 74.89 A/W, $4.22×10^{13}$ Jones, and $3.38×10^4\%$, respectively. The stable on-chip optical information transmission capability of the monolithically integrated photonic chips confirms the great potential for application in large-scale on-chip optical communication in the future.

**Keywords:** monolithically integration; photonic chips; UVC; solar-blind communication

## 1 Introduction

The rapid development of III-V nitride epitaxial growth technology has driven the advancement and application of multifunctional photoelectronic integrated devices based on nitride materials[1]. Due to the wide bandgap (6.2 eV~0.7 eV) of nitride materials, the corresponding nitride multiple quantum well (MQW) structure can cover wavelengths from deep ultraviolet to infrared[2]. Currently, the application of MQW structure light-emitting diodes (LED) is no longer limited to solid-state lighting but is gradually expanding into fields

such as biochemical detection, sensing, optical communication, optical computing, and displays[3 – 6]. As the core of future optical interconnects, on-chip optical communication technology consisting of light emission, transmission, and reception is becoming the key scientific technology driving the transition from on-chip electrical transmission to on-chip optical transmission[7 – 8]. The bonding processes introduced by traditional silicon-based heterogeneous integration technology significantly increase production costs, and low yield and high instability are also inevitable[9]. The epitaxial growth technology based on III-V nitride homogeneous integration can directly fabricate highly stable and multifunctional photonic integrated chips, providing a tremendous opportunity to advance on-chip optical communication technology.

In recent years, there have been numerous research reports on multifunctional on-chip integrated chips based on MQW structure light-emitting epitaxial wafers that can simultane-

ously achieve both emission and detection[10 – 13]. Unfortunately, the corresponding monolithic integrated photonic chips are mainly concentrated in the visible light band. The light emitted by visible light LEDs is divergent, which is not conducive to confining the optical signals within the integrated chip for on-chip optical communication. Moreover, the presence of unavoidable visible light in free environments necessitates consideration of how to avoid light noise interference when using visible light photonic integrated chips. In contrast, solar-blind photonic integrated chips have the following advantages: 1) The scattering of ultraviolet light by atmospheric particles creates a good application scenario free from ultraviolet light interference in ground-based free space. 2) Ultraviolet light is mainly composed of transverse magnetic (TM) modes, which is extremely beneficial for the lateral optical transmission of ultraviolet light signals within the integrated chips. 3) The carrier lifetime of deep ultraviolet light-emitting epitaxial wafers is lower, making it more advantageous to construct high-bandwidth photonic integrated chips for on-chip optical communication[14 – 16].

In this work, we successfully realize monolithically integrated chip fabrication of solar blind LEDs, waveguides, and PDs on an AlGaN MQW structure wafer. Combined with finite difference time domain (FDTD) simulation, the strong light constraint and advantages of horizontal transmission of solar blind TM modes are demonstrated. The photo-to-dark current ratio (PDCR) of the integrated self-driven PD is about seven orders of magnitude when the integrated LED is operated at 100 mA current. The responsivity, specific detectivity and external quantum efficiency (EQE) of the integrated self-driven PD are all excellent. This work will provide lots of experimental experience to promote the development of solar blind on-chip communication.

## 2 Experiment Details

The AlGaN-based ultraviolet-C (UVC) MQW structure epilayers are grown on 2-inch c-plane sapphire substrates using metal organic chemical vapor deposition (MOCVD). The designed UVC LED structure consists of 2.5 μm thick AlN, 20-period AlN/$Al_{0.6}Ga_{0.4}N$ SLs, a 2.0 μm n-$Al_{0.67}Ga_{0.33}N$ layer, a 1.3 μm n-$Al_{0.55}Ga_{0.45}N$ layer, 5-period $Al_{0.50}Ga_{0.50}N$/$Al_{0.37}Ga_{0.63}N$ MQWs, an about 30 nm superlattices-electron barrier layer (SLs-EBL), an about 20 nm graded p-AlGaN hole injection layer, and a 2 nm p-$Al_{0.2}Ga_{0.8}N$ contact layer.

Here, a novel SLs-EBL structure is specially designed to expand the potential field region and enhance the performance of the integrated device. More detailed design information on the SLs-EBL structure is presented in our previous related work[17]. Fig. 1a shows the optical transmission spectrum of the designed UVC LED structure. The well-defined oscillation curve demonstrates that the grown nitride epitaxial materials possess high quality. The growth of high-quality nitride epitaxy is fundamental to the fabrication of highly stable and uniform photonic integrated chips. The schematic diagram illustrates the physical mechanism of simultaneously achieving optical signal emission and reception using the same MQW structure LED epilayer in Fig. 1a. The one on the left is used as the integrated LED to emit light signals, and that on the right is used as the integrated PD to detect light signals. The part of photons from the integrated LED can be effectively absorbed by the integrated PD with the same MQWs structure. This phenomenon is caused by the partial overlap between the emission spectrum and the detection spectrum of the same MQW structure epilayer, as shown in Fig. 1b. The yellow shaded area represents the overlapping tail portion of the emission and detection spectra of the same MQW structure epilayer. This region provides the physical basis for constructing the on-chip optical information links. The excellent optoelectronic properties of the luminous epilayer are the necessary
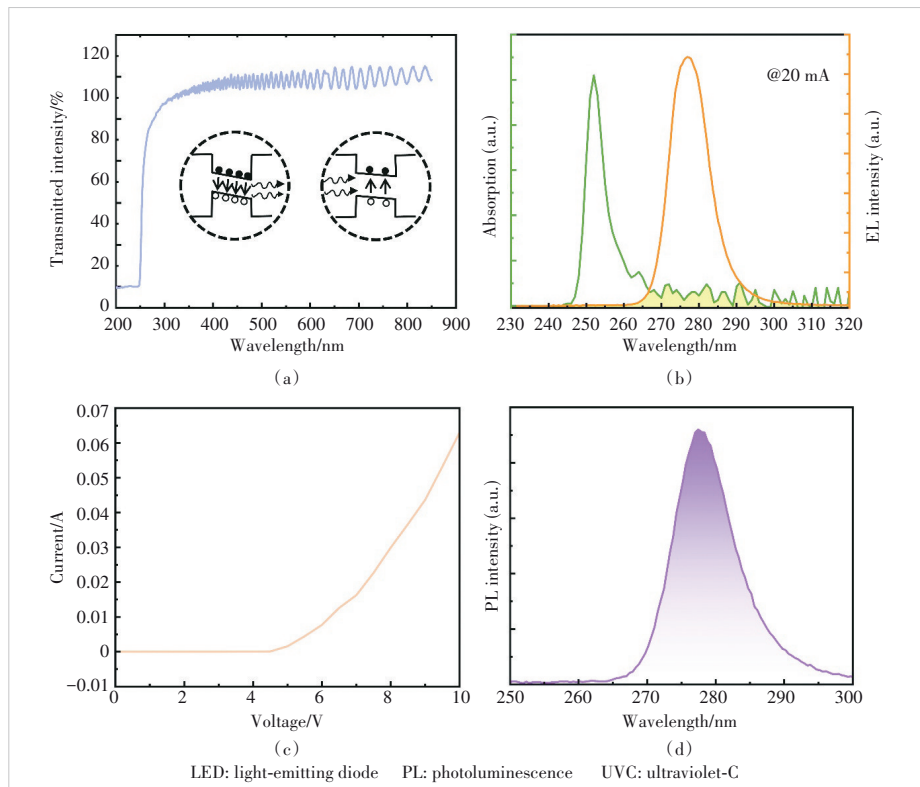


▲ Figure 1. (a) Optical transmission spectrum of the UVC LED epilayer, (b) absorption and EL spectra of the UVC LED epilayer, where the yellow shadow is the overlap region of these spectra, (c) I-V characteristic of the integrated LED, and (d) PL spectrum of LED epilayer

foundation for achieving efficient on-chip optical interconnects. Fig. 1c shows the I-V characteristic of the LED fabricated on the luminous epilayer with high quality. The low turn-on voltage implies reduced energy consumption. Furthermore, the photoluminescence (PL) spectrum in Fig. 1d shows an emission peak at approximately 277 nm, which falls within the solar-blind spectrum range. Ambient light causes minimal noise for solar-blind integrated chips, significantly broadening their application range, which is a major advantage of solar-blind integrated chips for future multifunctional large-scale integration applications.

The epilayer is fabricated as the monolithically integrated chips including integrated LEDs, waveguides, and PDs. Fig. 2 shows the fabrication processes of a monolithically integrated devices. Firstly, the mesa regions of the integrated LED and the integrated PD are defined by the inductively coupled plasma reactive ion etching (inductively coupled plasma-reactive ion etching, speed: 40 Å/s) with an etching depth of 500 nm. Secondly, Ti/Al/Ni/Au (20/60/30/100 nm) multi-layers are evaporated by an electron beam evaporator (EBE) and lifted off to form the p-contact metal electrodes of the integrated LED and integrated PD. Then the electrodes are treated by rapid thermal annealing (RTA) at 1 000 ℃ for 30 s in $N_2$ ambient to improve the ohmic contact performance. Similarly, Ni/Au (20/20 nm) multi-layers are deposited and lifted off to form the n-contact metal electrodes, followed by RTA at 700 ℃ for 1 min in $N_2$ atmosphere. Although two cathode electrodes are connected indirectly through the n-AlGaN layer, the integrated LED and PD work independently. Subsequently, the structure of the waveguide is defined by photolithography and transferred into the n-AlGaN layer through inductively coupled plasma (ICP) dry etching. It should be noted that for optimal optical confinement, the waveguides are vertically penetrated to the n-AlGaN layer with a depth of 2.5 μm. Finally, a high-quality
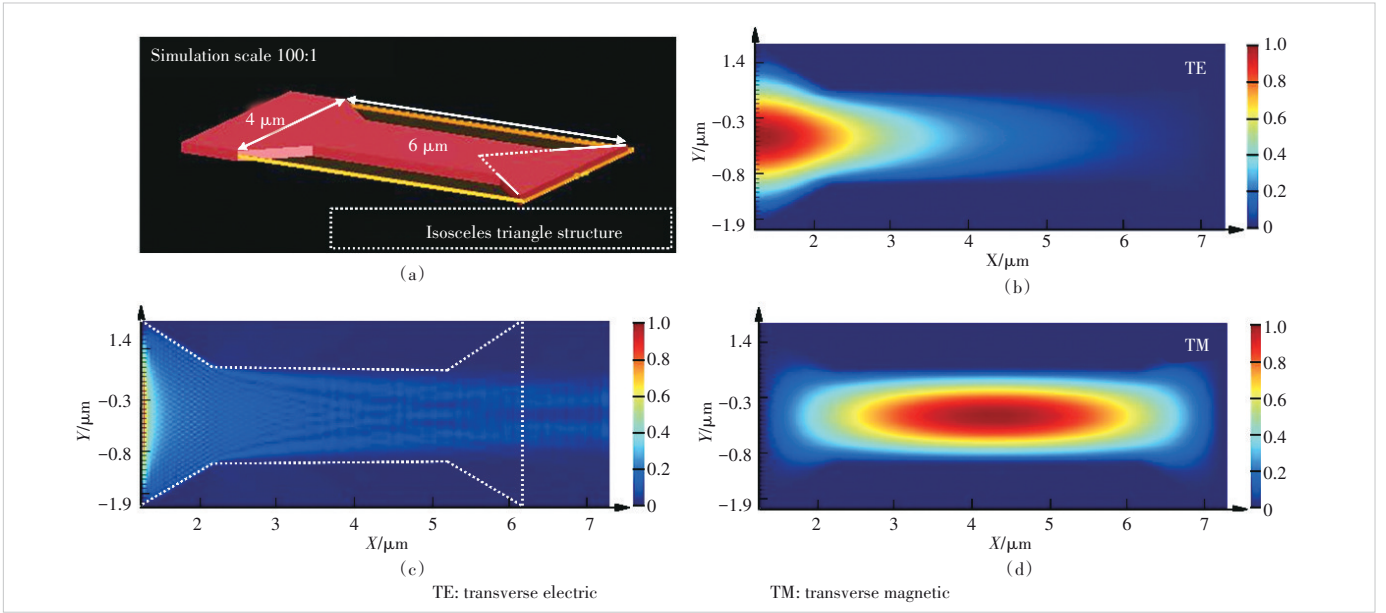
SiO$_2$ passivation protective layer with a thickness of 100 nm is deposited by plasma enhanced chemical vapor deposition (PECVD) and patterned by buffered oxide etch (BOE). It is important to emphasize that traditional ultraviolet LEDs use flip-chip packaging to allow more light to diverge, thereby improving light output efficiency. Here, we use gold wire bonding to package the monolithic integrated chips to better confine the ultraviolet light signal within the chip for lateral transmission, rather than allowing it to diverge.

## 3 Results and Discussions

FDTD simulation software is used to simulate the optical field distribution of the integrated waveguide. Fig. 3a presents the physical model of the integrated waveguide with an isosceles triangle structure. The simulation uses a scale of 100:1, so the actual waveguide length is 600 μm, and the base length of the triangle is 400 μm. Here, the refractive index for simulation is 2.42. Fig. 3b shows the optical field distribution when the optical signal propagates in the integrated waveguide. Due to the significant refractive index difference with the surrounding air environment, the integrated waveguide exhibits strong light confinement effects and demonstrates efficient optical information transmission capabilities. Furthermore, designing the waveguide structure as the isosceles triangle can further reduce optical crosstalk between adjacent devices during signal transmission, advancing the development of future large-scale photonic integration technology. We will further enhance the optical confinement of the integrated waveguide and strengthen the optical connection between the integrated LED and the integrated PD by optimizing the waveguide structure in subsequent work. Figs. 3c and 3d show the distribution of different mode light in the integrated waveguide. Notably, the TM mode light distributes better laterally in the integrated waveguide than the transverse electric (TE) mode light. It is well known that ultraviolet light is mainly composed of TM
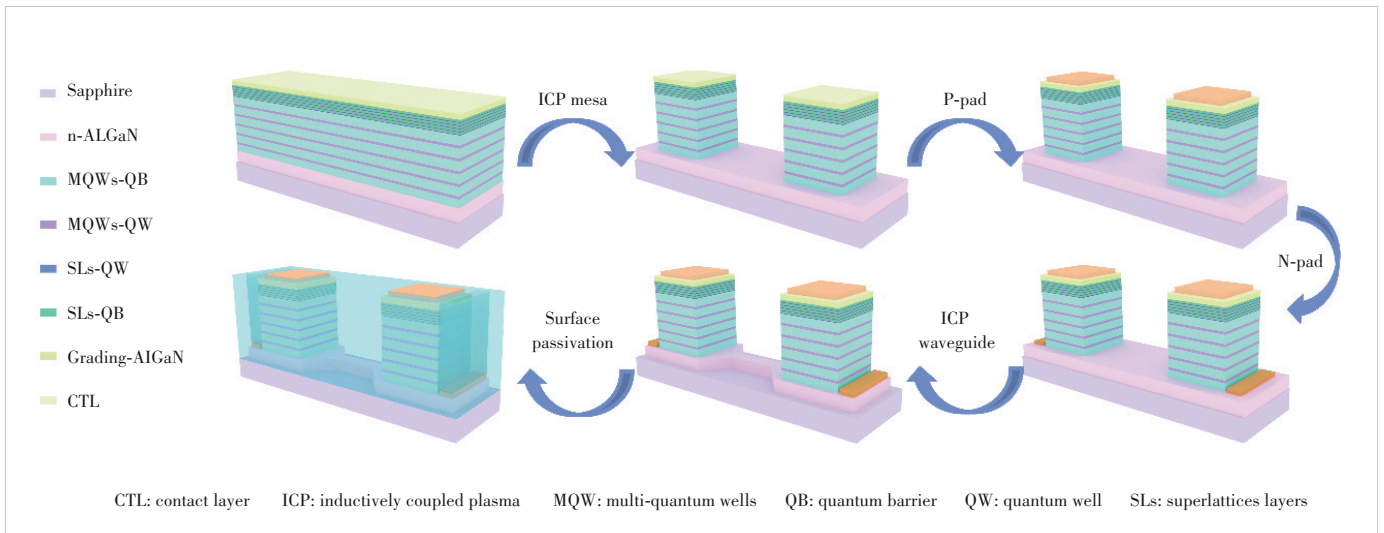


▲Figure 2. Fabrication processes of the monolithically integrated device using the designed UVC LED epilayer

CTL: contact layer    ICP: inductively coupled plasma    MQW: multi-quantum wells    QB: quantum barrier    QW: quantum well    SLs: superlattices layers

▲Figure 3. FDTD simulations of the waveguide structure: (a) schematic diagram of the simulated waveguide structure, (b) light field distribution in the n-AlGaN waveguide, (c) TE, and (d) TM modes distribution in the channel waveguide

modes that are more conducive to the lateral transmission of optical signals on-chip[18]. This is one of the main reasons why we choose solar-blind light for on-chip information transmission.

Fig. 4a shows the log-scaled current-voltage (I-V) plots for the integrated PD at the different injection current levels of the integrated LED from 0 mA to 100 mA. The dark currents under increased reverse bias voltages gradually increase from ~10 fA to ~1 nA due to high density dislocations in the AlGaN epilayer. However, as the injection current of the integrated LED is increased from 0 to 100 mA, the photocurrents of the integrated PD rise by about 7 orders of magnitude at 0 V bias. To quantify the response ability of the MQW structure PD, the responsivity $R$, specific detectivity $D^*$, and EQE are key parameters determined by the following equations[19-21].
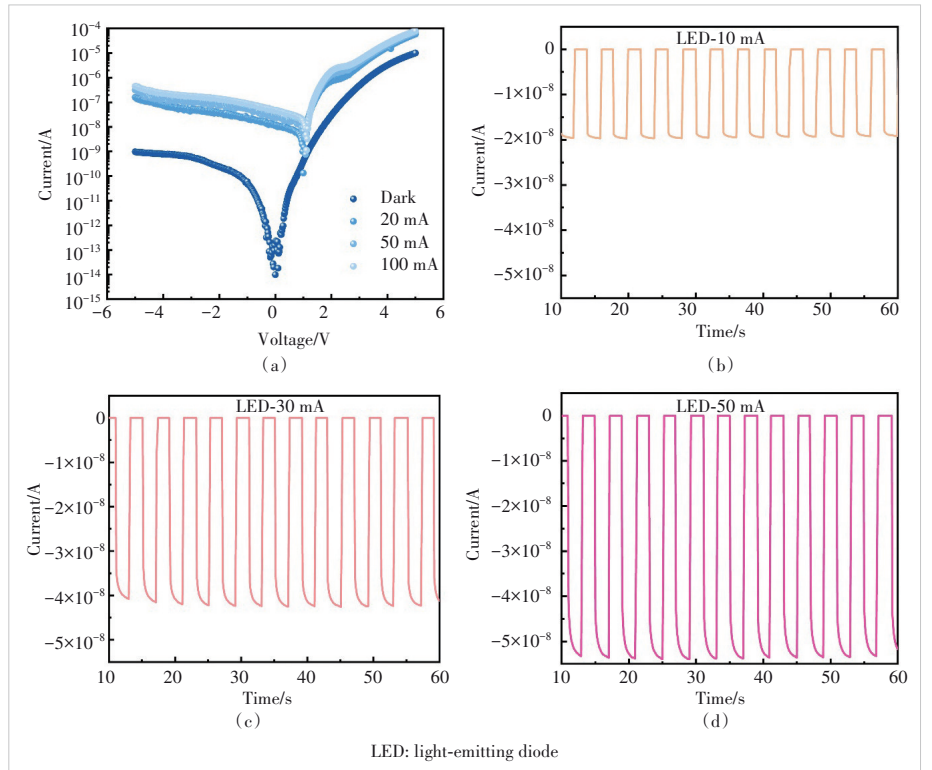
$$\Delta P = S \times I_P, \tag{1}$$

$$R = \frac{\Delta I}{\Delta P}, \tag{2}$$

$$D^* = \frac{\sqrt{A}\,R}{\sqrt{2eI_d}}, \tag{3}$$

$$EQE = \frac{hcR}{e\lambda}, \tag{4}$$

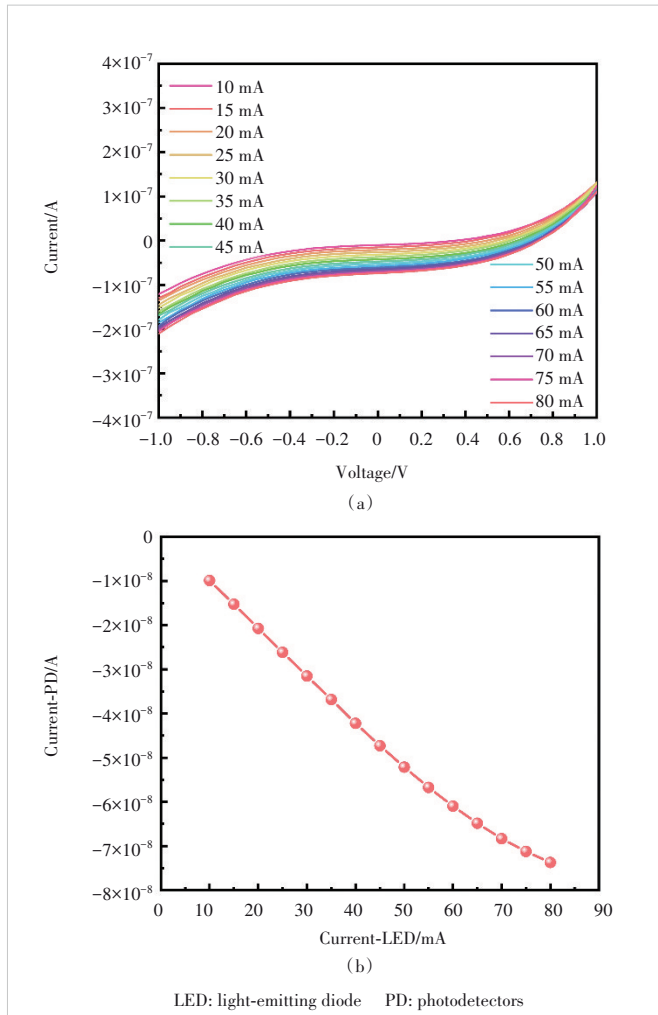where $S$ is the side wall area of the PD (about 1 000 $\mu m^2$), $I_P$



▲Figure 4. (a) I-V plots of the integrated PD responding to illumination from the integrated LED operated at currents from 0 (dark) to 100 mA; induced photocurrent temporal trace of the integrated PD at 0 V bias with the cyclical light changes in the integrated LED under (b) 10 mA, (c) 30 mA, and (d) 50 mA, respectively

is the optical power density, $\Delta I$ is the photocurrent (subtracting the dark-current from the photo-excited current), $\Delta P$ is the incident light intensity, $A$ is the effective illuminated area, $e$ is the elementary electric charge, $I_d$ is the dark-current, $h$ is Planck's constant, $c$ is the speed of light, and $\lambda$ is the incident light wavelength. For the integrated PD, the calculated $R$ is 74.89 A/W, $D^*$ is $4.22 \times 10^{13}$ Jones, and EQE is $3.38 \times 10^4$%. The time-resolved photocurrents of the integrated PD in response to the turn-on and turn-off state of the illumination from the integrated LED are shown in Figs. 4b – 4d. The currents applied to the integrated LED under the turn-on state are 10 mA, 30 mA, and 50 mA, respectively. The smooth and consistent signal response benefits from high PDCR and negligible thermal effect, demonstrating excellent response properties of the MQW structure PD.

Fig. 5a shows the I-V plots for the integrated PD at the different injection current levels of the integrated LED from 10 mA to 80 mA. Obviously, the photocurrent of the integrated PD will change with the change of the currents applied to the integrated LED indicating the stable optical link established between the integrated LED and the integrated PD. As depicted in Fig. 5b, the measured photocurrent of the integrated PD without voltage bias is directly proportional to the intensity of the incident current of the integrated LED, which is the prerequisite for stable work of the on-chip communication integration system. The integrated LED is used as the emitter, the integrated PD as the receiver, and the waveguide is used to build the optical bridge between the integrated LED and the integrated PD. The solar-blind monolithically photonic integrated chip integrating optical signal transmitter-waveguide-receivers is expected to construct a stable optical communication system without ambient light interference for large-scale on-chip optical interconnection and optical computing in the future.

## 4 Conclusions

In summary, the monolithically integrated photonic chips including LEDs, waveguides, and PDs are fabricated on the solar blind epilayer with the MQW structure. Because of the significant refractive index different from surrounding air, the waveguide shows excellent strong light constraint improving the transmission efficiency. Furthermore, the dominant TM modes in solar blind light are conducive to transverse optical transmission of optical signals along the waveguide inside the integrated chips. The PDCR of the integrated self-driven PD is about seven orders of magnitude when the integrated LED is operated at 100 mA current. The responsivity, specific detectivity and EQE of the integrated self-driven PD are all at an advanced level. This work will promote the application of solar-blind photonic integration technology, laying an experimental foundation for the development of high-quality high-speed on-chip optical communication technology in the future.

## Acknowledgement

▲Figure 5. (a) Photocurrents of the integrated PD responding to illumination from the integrated LED operated at currents from 10 mA to 100 mA; (b) change trend of the integrated PD photocurrent under different integrated LED injection currents

## References

[1] REN A B, WANG H, ZHANG W, et al. Emerging light-emitting diodes for next-generation data communications [J]. Nature electronics, 2021, 4(8): 559 – 572. DOI: 10.1038/s41928-021-00624-7

[2] LIANG D D, WEI T B, WANG J X, et al. Quasi van der Waals epitaxy nitride materials and devices on two dimension materials [J]. Nano energy, 2020, 69: 104463. DOI: 10.1016/j.nanoen.2020.104463

[3] KNEISSL M, SEONG T Y, HAN J, et al. The emergence and prospects of deep-ultraviolet light-emitting diode technologies [J]. Nature photonics, 2019, 13(4): 233 – 244. DOI: 10.1038/s41566-019-0359-9

[4] GUO L, GUO Y N, WANG J X, et al. Ultraviolet communication technique and its application [J]. Journal of semiconductors, 2021, 42(8): 081801.

DOI: 10.1088/1674-4926/42/8/081801

[5] YIN J H, YANG H Y, LUO Y M, et al. III-nitride microsensors for 360° angle detection [J]. IEEE electron device letters, 2022, 43(3): 458 – 461. DOI: 10.1109/LED.2022.3148232

[6] ZHANG H, YAN J B, YE Z Q, et al. Monolithic GaN optoelectronic system on a Si substrate [J]. Applied physics letters, 2022, 121(18): 181103. DOI: 10.1063/5.0125324

[7] LI K H, FU W Y, CHOI H W. Chip-scale GaN integration [J]. Progress in quantum electronics, 2020, 70: 100247. DOI: 10.1016/j. pquantelec.2020.100247

[8] SURYO W H, DANIEL P J, JAN G, et al. Beyond solid-state lighting: miniaturization, hybrid integration, and applications of GaN nano- and micro-LEDs [J]. Applied physics reviews, 2019, 6(4): 41315

[9] LIU A Y, BOWERS J. Photonic integration with epitaxial III – V on silicon [J]. IEEE journal of selected topics in quantum electronics, 2018, 24(6): 6000412. DOI: 10.1109/JSTQE.2018.2854542

[10] YAN L T, JIN Z X, LIN R Z, et al. InGaN micro-LED array with integrated emission and detection functions for color detection application [J]. Optics letters, 2023, 48(11): 2861 – 2864. DOI: 10.1364/OL.485939

[11] HE R, WANG L L, CHEN R F, et al. Monolithically integrated photonic chips with asymmetric MQWs structure for suppressing Stokes shift [J]. Applied physics letters, 2023, 122(2): 021105. DOI: 10.1063/5.0131115

[12] LI K H, FU W Y, CHEUNG Y F, et al. Monolithically integrated InGaN/GaN light-emitting diodes, photodetectors, and waveguides on Si substrate [J]. Optica, 2018, 5(5): 564. DOI: 10.1364/optica.5.000564

[13] ZHANG F H, SHI Z, GAO X M, et al. On-chip multicomponent system made with an InGaN directional coupler [J]. Optics letters, 2018, 43(8): 1874 – 1877

[14] GUO L, GUO Y N, YANG J K, et al. 275 nm deep ultraviolet AlGaN-based micro-LED arrays for ultraviolet communication [J]. IEEE photonics journal, 2022, 14(1): 8202905. DOI: 10.1109/JPHOT.2021.3129648

[15] SHAKYA J, KNABE K, KIM K H, et al. Polarization of III-nitride blue and ultraviolet light-emitting diodes [J]. Applied physics letters, 2005, 86 (9): 091107. DOI: 10.1063/1.1875751

[16] HE R, LIU N X, GAO Y Q, et al. Monolithically integrated UVC AlGaN-based multiple quantum wells structure and photonic chips for solar-blind communications [J]. Nano energy, 2022, 104: 107928. DOI: 10.1016/j.nanoen.2022.107928

[17] HE R, SONG Y J, LIU N X, et al. Solar-blind photonic integrated chips for real-time on-chip communication [J]. APL photonics, 2024, 9(7). DOI: 10.1063/5.0206657

[18] KOLBE T, KNAUER A, CHUA C, et al. Optical polarization characteristics of ultraviolet (In) (Al)GaN multiple quantum well light emitting diodes [J]. Applied physics letters, 2010, 97(17): 171105. DOI: 10.1063/1.3506585

[19] JIN Z W, GAO L, ZHOU Q, et al. High-performance flexible ultraviolet photoconductors based on solution-processed ultrathin ZnO/Au nanoparticle composite films [J]. Scientific reports, 2014, 4: 4268. DOI: 10.1038/srep04268

[20] RATHKANTHIWAR S, KALRA A, SOLANKE S V, et al. Gain mechanism and carrier transport in high responsivity AlGaN-based solar blind metal semiconductor metal photodetectors [J]. Journal of applied physics, 2017, 121(16): 164502. DOI: 10.1063/1.4982354

[21] HE R, WANG Y X, SONG Y J, et al. Selective area grown photonic integrated chips for completely suppressing the Stokes shift [J]. Applied physics letters, 2024, 124(25): 251103. DOI: 10.1063/5.0213979

## Biographies

**HE Rui** is now pursuing her PhD degree in the Institute of Semiconductors, Chinese Academy of Sciences. She received her BS degree in applied physics from University of Science and Technology Beijing, China. Her research mainly focuses on the research of optoelectronic integrated devices based on wide bandgap semiconductor materials.

**HU Qiang** is currently an associate professor in Research and Development Center for Wide Bandgap Semiconductors, Institute of Semiconductors, Chinese Academy of Sciences. His research interests focus on wide gap semiconductor MOCVD epitaxy and power devices.

**RAN Junxue** received his PhD degree from Institute of Semiconductors, Chinese Academy of Sciences in 2006. He is currently an associate professor in Research and Development Center for Wide Bandgap Semiconductors, Institute of Semiconductors, Chinese Academy of Sciences. His research interests focus on wide gap semiconductor MOCVD epitaxy and power devices.

**WANG Junxi** is currently a professor in materials physics and chemistry, Institute of Semiconductors, Chinese Academy of Sciences. He received his bachelor's degree in physics from Northwestern University, China in 1998, and his doctoral degree in engineering from Institute of Semiconductors, Chinese Academy of Sciences in 2003. His research interests focus on wide gap semiconductor material epitaxy, deep ultraviolet light-emitting diode (DUV-LED) devices, advanced semiconductor materials, and their applications.

**WEI Tongbo** (tbwei@semi.ac.cn) is currently a professor in materials physics and chemistry, Institute of Semiconductors, Chinese Academy of Sciences. He received his doctoral degree in engineering from the Institute of Semiconductors, Chinese Academy of Sciences in July 2007. His research interests focus on wide bandgap semiconductor materials and devices, new micronano photoelectronic devices, deep ultraviolet light emitting devices, and nitride growth on two-dimensional materials.